# Self-Assembled Monolayers of 7-(10-Thiodecoxy)coumarin on Gold: Synthesis, Characterization, and Photodimerization

**Weijin Li, Vincent Lynch, Heike Thompson, and Marye Anne Fox***

*Contribution from the Department of Chemistry and Biochemistry, The University of Texas at Austin, Austin, Texas 78712*

*Received February 26, 1997*[⊗]

**Abstract:** As is true in solution, irradiation at 350 nm of 7-(10-thiodecoxy)coumarin (**1**) as a self-assembled monolayer on polycrystalline gold (Au-**1**) produces [2 + 2] photodimers. In the monolayer, photodimerization is indicated by differences in the grazing angle surface FTIR spectra, sessile drop contact angles, and surface fluorescence spectra before and after irradiation. The photodimerization can be reversed by irradiation at 254 nm, as demonstrated by changes in these same structural probes. Better photochemical reversibility and regioselectivity are observed when the *in situ* photodimerization is conducted as a dry solid monolayer than when in contact with benzene. A comparison of the structure of a self-assembled monolayer of a *syn* head-to-head (H-H) dimer of 7-(10-thiodecoxy)coumarin on polycrystalline gold (Au-**2**) with that of the photodimers generated by irradiation of Au-**1** demonstrates that surface reorganization is accomplished in the photodimerization−photoreversion cycle.

## Introduction

Photodimerization of coumarin and its derivatives has been extensively studied in homogeneous solution[1,2] and in organized media such as micelles,[3−6] cyclodextrin inclusion complexes,[7] and crystals.[7−10] Upon irradiation with wavelengths longer than 300 nm in solution, coumarin derivatives are generally converted to four regioisomeric photodimers (the *syn* head-to-head (H-H), *syn* head-to-tail (H-T), *anti* head-to-head, and *anti* head-to-tail dimers) through a [2 + 2] photocycloaddition, as shown in Scheme 1 for 7-(10-thiodecoxy)coumarin.[11] These photodimers can be photocleaved upon irradiation at wavelengths shorter than 300 nm.[11] Photochemical reversibility has also been demonstrated in polymers bearing pendent coumarin chromophores and in a series of 7-alkoxycoumarin derivatives dispersed in a polymer matrix.[12]

**Scheme 1**

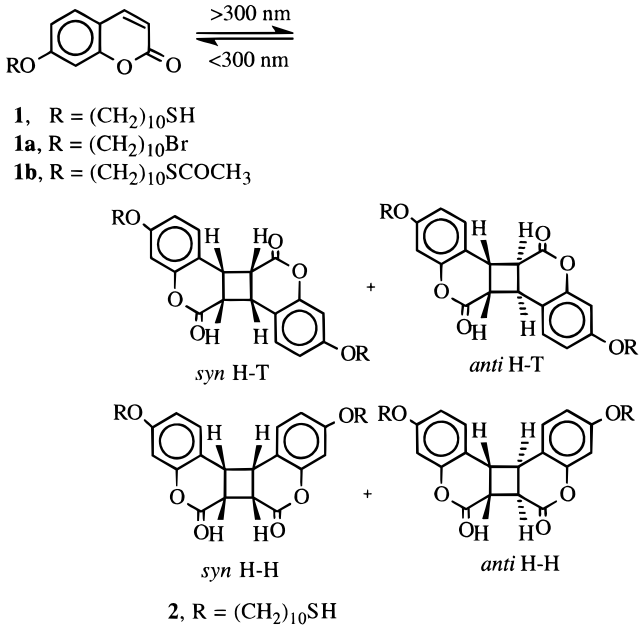


An interesting property associated with 7-alkoxycoumarin photodimerization is the modulation of fluorescence emission. Upon excitation at 320 nm, 7-alkoxycoumarin strongly fluoresces, whereas the corresponding dimers do not.[11] Therefore, these simple photodimerization and photocleavage reactions represent an on−off fluorescence switch that might allow reversible photomodulation of an observable electronic property. This external light trigger thus constitutes a basic component of a potential photonic imaging device.[13] For practical device applications, it is desirable to determine whether such photochemical behavior is also observable in thin layers.

We report in this study the preparation, characterization, and photochemistry of a photoactive coumarin derivative, 7-(10-thiodecoxy)coumarin (**1**), in solution and as a self-assembled monolayer (SAM) on polycrystalline Au. We demonstrate that

[⊗] Abstract published in *Advance ACS Abstracts,* July 15, 1997.

(1) Leenders, L. H.; Schouteden, E.; Schryver, F. C. D. *J. Org. Chem.* **1973**, *38*, 957.
(2) Morrison, H. H.; Curtis, H.; McDowell, T. *J. Am. Chem. Soc.* **1966**, *88*, 5415.
(3) Muthuramu, K.; Ramamurthy, V. *J. Org. Chem.* **1982**, *47*, 3976.
(4) Muthuramu, K.; Ramnath, N.; Ramamurthy, V. *J. Org. Chem.* **1983**, *48*, 1872.
(5) Muthuramu, K.; Ramamurthy, V. *Ind. J. Chem.* **1984**, *23B*, 502.
(6) Marques, A. D. S.; Marques, G. S. S. *Photochem. Photobiol.* **1994**, *59*, 153.
(7) Moorthy, J. N.; Venkatesan, K.; Weiss, R. G. *J. Org. Chem.* **1992**, *57*, 3292.
(8) Bhadbhade, M. M.; Murthy, G. S.; Venkatesan, K.; Ramamurthy, V. *Chem. Phys. Lett.* **1984**, *109*, 259.
(9) Gnanaguru, K.; Ramasubbu, N.; Venkatesan, K.; Ramamurthy, V. *J. Org. Chem.* **1985**, *50*, 2337. Systematic studies by Ramamurthy and others on the photodimerization of coumarins have shown that the cyclobutyl protons of coumarin *syn* dimers appeared as two multiplets (2 H each) centered around $\delta$ 4.0 and 4.2, whereas those in the coumarin *anti* dimers resonate as a multiplet (4 H) below $\delta$ 3.9. Here, the cyclobutyl protons appear as two multiplets centered at $\delta$ 3.96 and 4.05 and are therefore assigned to a *syn* dimer. Coumarin *syn* H-T dimers (such as that of 7-methoxycoumarin) also have a characteristic upfield (>0.6 ppm) $H_8$ proton, deriving from the diamagnetic anisotropy caused by a phenyl ring situated in front of the $H_8$ proton.
(10) Stitchell, S. G.; Harris, K. D. M.; Aliev, A. E. *Struct. Chem.* **1994**, *5*, 327.
(11) Kuznetsova, N. A.; Kaliya, O. L. *Russ. Chem. Rev.* **1992**, *61*, 683.
(12) (a) Chen, Y.; Wu, J.-D. *J. Polym. Sci., Polym. Chem. Ed.* **1994**, *32*, 1867. (b) Chen, Y.; Chou, C.-F. *J. Polym. Sci., Polym. Chem. Ed.* **1995**, *33*, 2705.
(13) Tsivgoulis, G. M.; Lehn, J.-M. *Angew. Chem., Int. Ed. Engl.* **1995**, *34*, 1119.

S0002-7863(97)00633-1 CCC: $14.00 

the well-known reversible photodimerization of a coumarin derivative (here of **1**) can be extended to these self-assembled monolayers, as established by cyclic voltammetry, sessile drop contact angle measurements, grazing angle surface FTIR spectra, and surface fluorescence measurements. As with previous photochemical studies of organic molecules tethered at the outer edge of self-assembled monolayers[14] and of some adsorbates on metals,[15] photochemical conversions are observed despite competition with quenching by the gold surface.[16]

In addition, we examine local ordering on the surface by comparing the properties of a self-assembled monolayer of preformed dimer on gold (Au-**2**) with the array produced by *in situ* photodimerization of Au-**1**. Our further goal is to study the photochemical reversibility of a fluorescent switch on a metal surface and to demonstrate whether the emission of the attached chromophore can be used for nondestructive surface patterning in a write−erase device. This area has been subject to extensive investigation recently in applications such as photonic molecular devices, photomemory materials, and photopatterning of gold surfaces.[14] However, much of the currently available research involves irreversible ablation of the irradiated component of the monolayer,[17] making many of the surfaces studied so far unsuitable for erasing and rewriting.

## Experimental Section

**General Procedures.** A gold-coated silicon (Silicon Sense Inc.) wafer was prepared by sequential thermal deposition of a 60 Å layer of chromium (to enhance the adhesion), followed by a 2000 Å layer of gold (99.99%). The gold-coated wafer was washed sequentially with hexane, $CH_2Cl_2$, and ethanol. Au-**1** was prepared by immersing the wafer in a dilute solution of **1** in ethanol (1 mM) at room temperature until no further changes in contact angle or cyclic voltammetry measurements could be observed (10 days). The modified surfaces were then rinsed repeatedly with ethanol and dried under a slow stream of Ar. The gold plates used in the electrochemical measurements had identical surface areas (0.72 $cm^2$), which was assured by using a copper mask.

The same procedure was followed for preparation of Au-**2**, except that $CH_2Cl_2$ was used as solvent with a immersion−equilibration period of 2 weeks. Although very high purity alkanethiols are not required to obtain reproducible results,[18] 7-(10-thiodecoxy)coumarin **1** and its dimer **2** used in this study were analytically pure (>99%).

A Rayonet photochemical reactor (Southern New England Ultraviolet Co.), fitted with a set of RUL lamps with broad emissions that are maximal at 3500 Å or at 3000 Å, was used in the photodimerization and the photocleavage. Under an atmosphere of $N_2$ or in contact with $N_2$-saturated benzene, photodimerization of the monolayers on gold was carried out inside a Pyrex test tube, whereas photocleavage was accomplished inside a quartz photoreactor.

Melting points were measured by a Melt-Temp apparatus (uncorrected). Nuclear magnetic resonance (NMR) spectra were recorded on a Bruker AC-250 (250 MHz) spectrometer. Chemical shifts are reported as $\delta$ values relative to an internal standard. High-resolution mass spectra were recorded on a VGZAB2-E (VG Analytical LTD., Manchester, U.K.) mass spectrometer. Fast atom bombardment (FAB) mass spectra were recorded on a Finnigan TSQ 70 instrument with the sample in a 3-nitrobenzyl alcohol (NBA) matrix.

Transmission FTIR spectra were recorded on a Nicolet 510P FT-IR spectrometer. Grazing angle surface FTIR spectra of SAMs on Au were obtained on a Nicolet Magna-IR spectrometer using p-polarized light at an angle of incidence of 87°, equipped with a liquid-nitrogen-cooled MCT/A detector. Typically, 512 scans at 4 $cm^{-1}$ resolution were collected. Background spectra were collected immediately before every measurement. Peak positions are determined as averages of spectra from five independent measurements of separate samples and are accurate to within 1 $cm^{-1}$.

**Scheme 2**

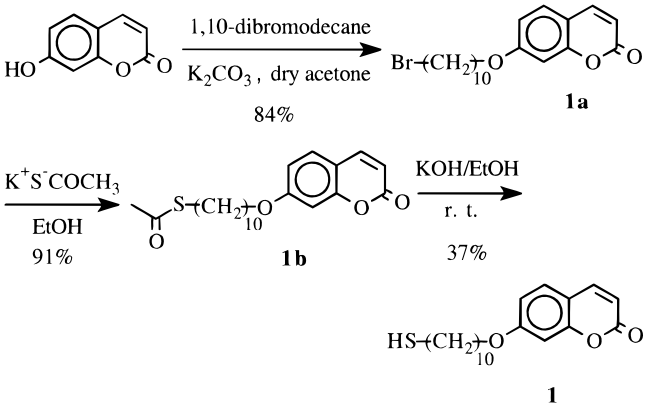


Cyclic voltammetry was used to investigate the integrity of the Au-**1** and Au-**2** SAMs. $Fe(CN)_6^{3-}/Fe(CN)_6^{4-}$, a well-known and electrochemically reversible, single-electron, outer-sphere redox pair,[19] was used as the probe redox pair. Electrochemical measurements were performed on a Princeton Applied Research 173 potentiostat, with a saturated calomel reference electrode (SCE). The modified gold plates Au-**1** and Au-**2** described above were employed as working electrodes in an aqueous solution of 1 mM $K_3Fe(CN)_6$ in aqueous 1 M KCl, with a Pt flag (about 0.5 $cm^2$) as counterelectrode. Millipore (Milli-Q-grade) water was used as solvent.

Contact angles were determined on a Rame-Hart Model 100 goniometer under ambient lab conditions.[18] X-ray data were collected at 183 K on a Siemens P4 diffractometer, equipped with a Nicolet LT-2 low-temperature device and a graphite monochromator with Mo K$\alpha$ radiation ($\lambda$ = 0.710 73 Å). Absorption spectra were recorded on a Shimadzu UV-3101 scanning spectrophotometer. Solution fluorescence spectra were recorded on a SLM Aminco SPF-500C spectrofluorometer, having been deoxygenated by bubbling with Ar for 20 min.

Surface fluorescence spectra of SAMs on Au were collected on a SPEX Fluorolog 2 instrument in the front face mode with samples mounted in an identical position. The instrument contains a 450 W Xe lamp, a Hammamatsu R508 photomultiplier, and double-grating monochrometers on both excitation and emission sides of the sample compartment. The spectra were collected on a SPEX DM3000 controller unit interfaced with the Fluorolog instrument with samples held in a special custom-designed sample holder that places the gold plate sample at a fixed distance from the excitation source and detector, allowing reproducible fluorescence intensities to be recorded. All surface fluorescence spectra were corrected for background emission from bare gold.

**Synthesis.** Literature methods[15,20] were successfully employed to prepare 7-(10-(thioacetyl)decoxy)coumarin in high yield (Scheme 2), but cleavage of the acetyl group by the previously described method was unsuccessful.[15] To suppress the undesirable side polymerization, a dilute solution of KOH in ethanol (0.2 N) was used as limiting reagent (0.7 equiv) for the hydrolysis, producing a 37% yield of **1**.

7-Hydroxycoumarin, 1,10-dibromodecane, and potassium thioacetate were purchased from Aldrich and used as received. Dry acetone was freshly distilled from anhydrous $CaSO_4$.

**7-(10-Bromodecoxy)coumarin (1a).** A solution of 7-hydroxycoumarin (6.0 g, 37 mmol), 1,10-dibromodecane (33 g, 110 mmol), and anhydrous $K_2CO_3$ (10 g, 72 mmol) in dry acetone (100 mL) was heated to reflux for 48 h. After the solvent was removed *in vacuo*, water was added, and the residue was extracted with $CH_2Cl_2$ (3 × 100 mL). The extract was dried over anhydrous $MgSO_4$, filtered, and evaporated *in*

(14) (a) Wolf, M. O.; Fox, M. A. *J. Am. Chem. Soc.* **1995**, *117*, 1845. (b) Wolf, M. O.; Fox, M. A. *Langmuir* **1996**, *12*, 955.

(15) (a) Zhou, X.-L.; Zhu, X.-Y.; White, J. M. *Acc. Chem. Res.* **1990**, *23*, 327. (b) Zhou, X.-L.; Zhu, X.-Y.; White, J. M. *Surf. Sci. Rep.* **1991**, *13*, 77.

(16) (a) Whitmore, P. M.; Robota, H. J.; Harris, C. B. *J. Chem. Phys.* **1982**, *77*, 1560. (b) Waldeck, D. H.; Alivisatos, A. P.; Harris, C. B. *Surf. Sci.* **1985**, *158*, 103.

(17) Wollman, E. W.; Kang, D.; Frisbie, C. D.; Lorkovic, I. M.; Wrighton, M. S. *J. Am. Chem. Soc.* **1994**, *116*, 4395.

(18) Bain, G. D.; Troughton, E. B.; Tao, Y.-T.; Evall, J.; Whitesides, G. M.; Nuzzo, R. G. *J. Am. Chem. Soc.* **1989**, *111*, 321.

(19) Bard, A. J.; Faulkner, L. R. *Electrochemical Methods: Fundamentals and Applications*; Wiley: New York, 1980.

(20) Allen, C. F. H.; Gates, J. J. W. *Organic Syntheses;* Wiley: New York, 1955; Collect. Vol. III, p 140.

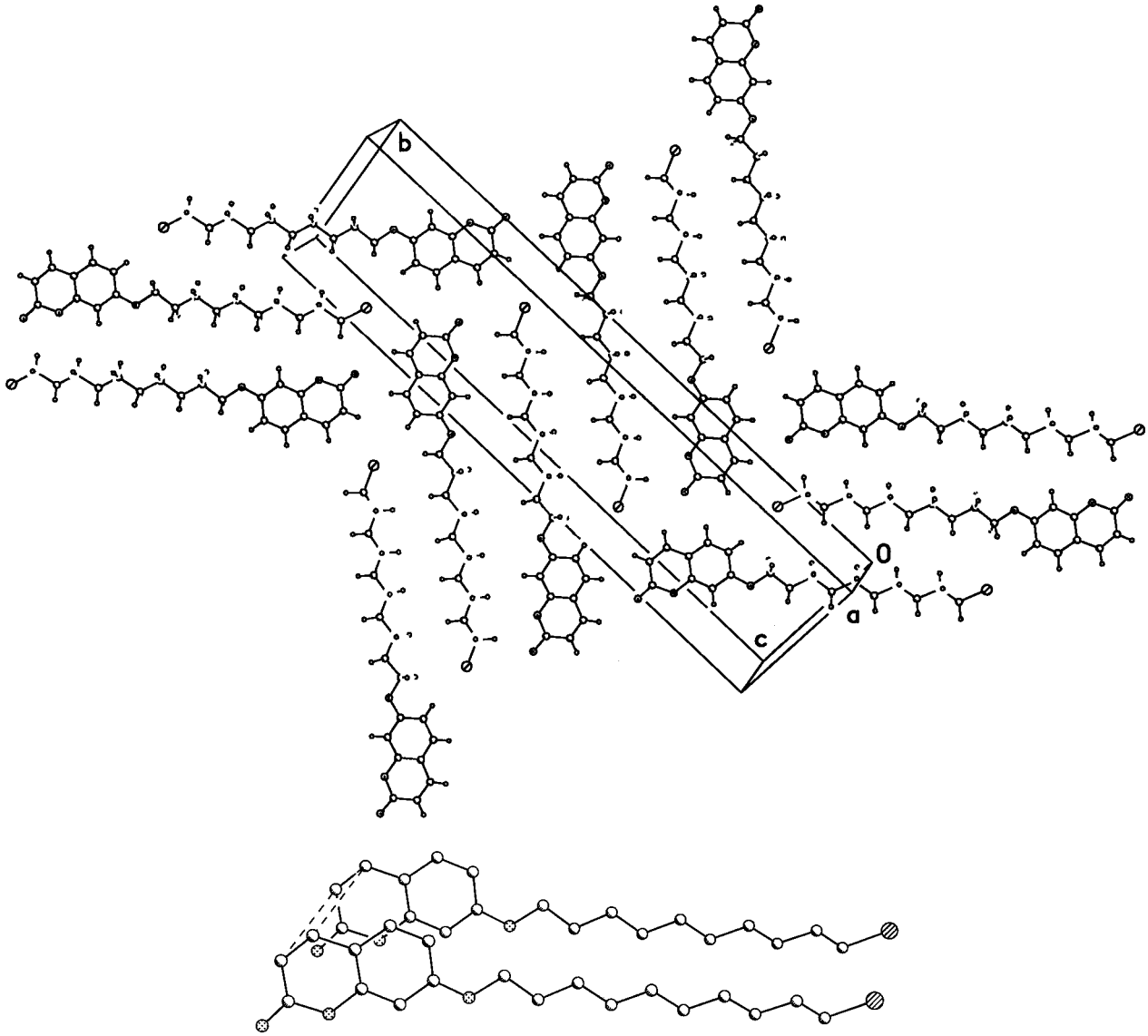


**Figure 1.** Packing arrangement of crystalline 7-(10-thiodecoxy)coumarin (**1**) (top) and disposition of a pair of monomers with the reactive double bonds $C_3-C_4$ and $C_3'-C_4'$ connected by dash lines (bottom).

*vacuo*. The residue was then chromotographed on silica gel eluted with chloroform−hexane (1:1) to afford 12 g (84%) of a white solid: mp 76−77 °C; $^1$H NMR ($CDCl_3$) $\delta$ 7.59 (d, $J$ = 9.5 Hz, 1 H), 7.33 (d, $J$ = 8.5 Hz, 1 H), 6.80 (dd, $J$ = 8.5 Hz, 2.4 Hz, 1 H), 6.77 (d, $J$ = 2.4 Hz, 1 H), 6.21 (d, $J$ = 9.5 Hz, 1 H), 3.98 (t, $J$ = 6.5 Hz, 2 H), 3.38 (t, $J$ = 6.8 Hz, 2 H), 1.85−1.81 (m, 4 H), 1.79−1.29 (m, 12 H); $^{13}$C NMR ($CDCl_3$) $\delta$ 162.4, 161.2, 155.9, 143.4, 128.7, 112.9, 112.9, 112.3, 101.3, 68.6, 34.0, 32.8, 29.3, 29.3, 29.2, 28.9, 28.7, 28.1, 25.9; HRMS (*m*/*z*) calcd for $(C_{19}H_{25}O_3Br + H)^+$ 381.1056, found 381.1065.

**7-(10-(Thioacetyl)decoxy)coumarin (1b).** A solution of 7-(10-bromodecoxy)coumarin (4.0 g, 11 mmol) and potassium thioacetate (1.3 g, 11 mmol) in 100 mL of absolute ethanol was heated to reflux for 24 h. The solvent was then removed *in vacuo*, and the residue was dissolved in $CH_2Cl_2$ and washed with water (3 × 100 mL). The extract was dried over anhydrous $MgSO_4$, filtered, and evaporated *in vacuo* to afford 3.6 g (91%) of an off-white solid: mp 58−59 °C; $^1$H NMR ($CDCl_3$) $\delta$ 7.59 (d, $J$ = 9.5 Hz, 1 H), 7.33 (d, $J$ = 8.5 Hz, 1 H), 6.80 (dd, $J$ = 8.5 Hz, 2.4 Hz, 1 H), 6.77 (d, $J$ = 2.4 Hz, 1 H), 6.21 (d, $J$ = 9.5 Hz, 1 H), 3.98 (t, $J$ = 6.5 Hz, 2 H), 2.83 (t, $J$ = 7.3 Hz, 2 H), 2.29 (s, 3 H), 1.83−1.72 (m, 2 H), 1.63−1.28 (m, 14 H); $^{13}$C NMR ($CDCl_3$) $\delta$ 195.9, 162.3, 161.1, 155.8, 143.3, 128.5, 112.8, 112.8, 112.2, 101.2, 68.5, 30.5, 29.3, 29.3, 29.2, 29.1, 29.0, 28.9, 28.8, 28.6, 25.8; HRMS (*m*/*z*) calcd for $(C_{21}H_{28}O_4S + H)^+$ 377.1795, found 377.1787.

**7-(10-Thiodecoxy)coumarin (1).** A solution of KOH (0.2 N) in ethanol (15 mL, 3.0 mmol) was added to a solution of 7-(10-(thioacetyl)decoxy)coumarin (1.6 g, 4.3 mmol) in ethanol (100 mL) over the period of 10 min at room temperature (rt). The reaction mixture was stirred at rt for another 5 min, and then the reaction was quenched by adding several drops of acetic acid. After solvent was removed, water was added to the mixture, and the residue was extracted by $CH_2Cl_2$ (3 × 100 mL). The extract was washed with water (3 × 100 mL) and dried over $MgSO_4$ (anhydrous), filtered, and evaporated *in vacuo*. The residue was then chromotagraphed on silica gel eluted with chloroform to give 0.37 g (37%, based on KOH) of an off-white solid (**1**): mp 62−63 °C; $^1$H NMR ($CDCl_3$) $\delta$ 7.59 (d, $J$ = 9.5 Hz, 1 H, $H_3$), 7.33 (d, $J$ = 8.5 Hz, 1 H, $H_5$), 6.80 (dd, $J$ = 8.5, 2.4 Hz, 1 H, $H_6$), 6.77 (d, $J$ = 2.4 Hz, 1 H, $H_8$), 6.21 (d, $J$ = 9.5 Hz, 1 H, $H_4$), 3.97 (t, $J$ = 6.5 Hz, 2 H), 2.49 (dd, $J$ = 7.4, 14.6 Hz, 2 H), 1.83−1.72 (m, 2 H), 1.63−1.52 (m, 2 H), 1.46−1.22 (m, 12 H); $^{13}$C NMR ($CDCl_3$) $\delta$ 162.4, 161.2, 155.9, 143.4, 128.7, 113.0, 112.9, 112.3, 101.3, 68.6, 34.0, 29.4, 29.4, 29.2, 29.0, 28.9, 28.3, 25.9, 24.6; HRMS (*m*/*z*) calcd for $(C_{19}H_{26}O_3S + H)^+$ 335.1692, found 335.1681; fluorescence emission ($CH_2Cl_2$) $\lambda_{max}$ 384 nm.

**Photodimerization of 1 in Solid State.** Crystalline **1** packs in $\beta$-stacks (Figure 1, top), such that the two ring double bonds ($C_3-C_4$ and $C_3'-C_4'$) are positioned parallel to each other with a center−center distance of 4.121 Å (Figure 1, bottom). The translational relations between the two double bonds are $\theta 1 = 0°$, $\theta 2 = 122.7°$, and $\theta 3 = 88.9°$.[9] The X-ray crystal structure of **1** suggests that only one geometry for the photodimer, a *syn* H-H dimer, should be favorable topochemically in the solid state.[9]

Single-crystal powders were used for the photodimerization using a literature method.[9] During the photodimerization, the white crystals turned brownish, indicating partial decomposition of **1**. Therefore, the

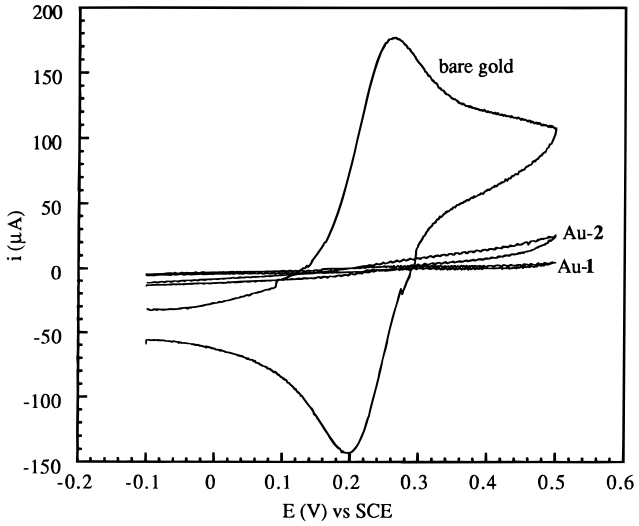


**Figure 2.** Cyclic voltammetric current response of a degassed solution of 1 mM $K_3Fe(CN)_6$ in aqueous 1 M KCl on bare gold, on Au-**1**, and on Au-**2** at room temperature. The sweep rate is 100 mV/s.

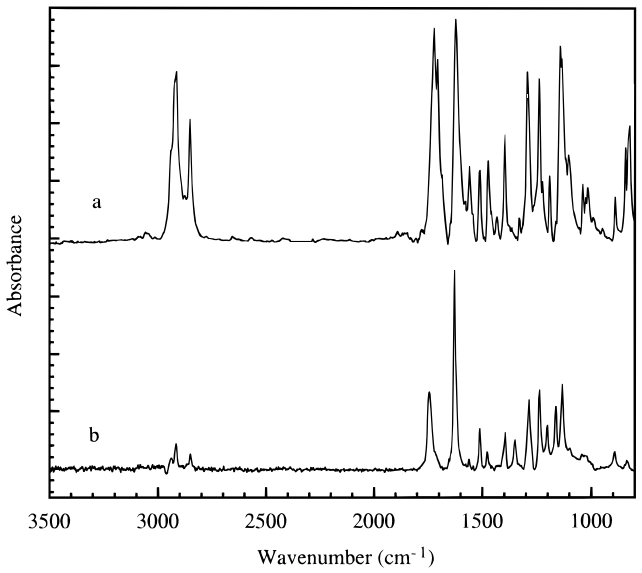


**Figure 3.** FTIR spectra of **1**: (a) dispersed in a KBr pellet and (b) as a SAM on Au.

reaction was allowed to proceed only to a 40−50% conversion of monomer. One major dimer was isolated by preparative TLC using $CHCl_3$ as eluent. The stereochemistry of the dimer was assigned by analyzing the patterns and the chemical shifts of the cyclobutyl protons.[9] Because the $H_8$ proton in the isolated dimer is upfield by 0.38 ppm, the solid-state photodimer is therefore assigned to a *syn* H-H dimer, as was expected from a topochemical analysis of its crystal packing.

**7-(10-Thiodecoxy)coumarin dimer (2).** Powdered single crystals of 7-(10-thiodecoxy)coumarin (100 mg) dispersed in a Pyrex test tube were irradiated with a Rayonet photochemical reactor fitted with a set of RUL lamps with emission maximized at 3500 Å for 24 h under an atmosphere of $N_2$. Samples were rotated periodically during irradiation to provide uniform exposure. The major dimer was separated by preparative TLC (silica gel) using $CHCl_3$ as eluent to afford 15.6 mg of *syn* H-H dimer (**2**): $^1$H NMR ($CDCl_3$) $\delta$ 6.65 (d, $J$ = 8.5 Hz, 2 H), 6.48 (dd, $J$ = 8.5, 2.5 Hz, 2 H), 6.39 (d, $J$ = 2.5 Hz, 2 H), 4.05 (m, 2 H), 3.96 (m, 2 H), 3.84 (t, $J$ = 6.5 Hz, 4 H), 2.50 (dd, $J$ = 7.4, 14.6 Hz, 4 H), 1.74−1.23 (m, 32 H); $^{13}$C NMR ($CDCl_3$) $\delta$ 164.5, 159.9, 152.8, 129.3, 111.9, 108.4, 102.4, 68.1, 39.6, 33.9, 29.3, 29.3, 28.9, 28.2, 25.8, 24.5; HRMS (*m*/*z*) calcd for $(C_{38}H_{52}O_6S_2 + H)^+$ 669.3284, found 669.3293.

## Results and Discussion

**Electrochemical Measurements.** Figure 2 shows the cyclic voltammetry of 1 mM $Fe(CN)_6^{3-}$ on bare gold, Au-**1**, and Au-**2** with 1 M KCl aqueous solution as electrolyte. On bare gold, the shape of the current−voltage curve and the 60 mV separation between $E_{p,c}$ and $E_{p,a}$ indicates a diffusion-limited, electrochemically reversible one-electron redox process.[19] On the other hand, cyclic voltammetry curves for Au-**1** and Au-**2** are dramatically different. The observed current at the modified electrodes is suppressed by a factor of $>10^3$ compared with bare gold with identical surface area, surface structure, and surface cleanliness. The fact that the current observed on Au-**2** is higher than that on Au-**1** suggests that Au-**2** is somewhat less densely packed than Au-**1**. The lower packing density in Au-**2** could be rationalized if adsorbate **2**, during the self-assembly process,[18] was less able to displace included solvent molecules or contaminants than adsorbate **1**. This would result in a much lower packing density in Au-**2**.

The progress of the self-assembly of **1** onto the gold surface can be followed by electrochemistry. After 2 days of immersion of a freshly deposited Au wafer into an ethanol solution of **1**, the oxidation peak for $Fe(CN)_6^{4-}$ is totally suppressed and the attenuated reduction peak shifts to a more negative potential. These same shifts continue for 10 days, after which no further changes could be observed. Compared with the self-assembly of alkanethiols on gold, which usually requires less than several hours,[18] the self-assembly of **1** on gold is unexpectedly slow, probably because of the bulky coumarin head group.[21]

Total blocking of $Fe(CN)_6^{3-}/Fe(CN)_6^{4-}$ redox chemistry was observed when Au-**1**, prepared by immersing the gold plate in **1** solution for 4 days, was irradiated at 350 nm for 10 h. Furthermore, when the same $(Au\text{-}\mathbf{1})_{dimer}$ plate was subject to cleavage by irradiation at 300 nm for 30 min, no further CV change could be observed. A control experiment was conducted to evaluate possible thermal origins of this effect. No CV change could be induced by heating Au-**1** at 40 °C (the temperature of the irradiation under our experimental conditions is <35 °C) for 2 h. We surmise that reorganization, most probably of the relative orientation of coumarin rings, takes place during the photodimerization and that the reordered surface is retained after photocleavage. The surface obtained by photocleavage of $(Au\text{-}\mathbf{1})_{dimer}$ differs significantly from that obtained with Au-**1**, presumably because the coumarin rings of the surface-confined monomers generated by reversion of the photodimer remain in a close-packed, face-to-face conformation.

Thus, strong specific interactions between the terminal thiol group and the gold surface result in spontaneous self-assembly of monolayers of **1** or **2** on the surface. The long alkyl chain ends of **1** adopt a dense packing, forming an insulating, pinhole-free[22,23] organic thin film that blocks the solution phase redox chemistry of $Fe(CN)_6^{3-}/Fe(CN)_6^{4-}$.

**Infrared Spectroscopy Studies.** Grazing angle surface FTIR spectroscopy was employed to further characterize the structure of Au-**1**. The grazing angle surface FTIR spectra of Au-**1** is compared with the transmission FTIR spectrum of bulk **1** dispersed in a KBr pellet in Figure 3. Characteristic peaks of both spectra are summarized in Table 1, with spectral assignments have been made by comparison with similar structures.[24−27] Several differences are evident between the transmission IR

(21) Echegoyen, L.; Kaifer, A. E. *Physical Supramolecular Chemistry*; Kluwer Academic Publisher: Amsterdam, 1996, p. 143.
(22) Chidsey, C. E. D.; Loiacono, D. N. *Langmuir* **1990**, *6*, 682.
(23) Finklea, H. O.; Snider, D. A.; Fedyk, J.; Sabatani, E.; Gafni, Y.; Rubenstein, I. *Langmuir* **1993**, *9*, 3660.
(24) Socrates, G. *Infrared Characteristic Group Frequencies: Tables and Charts*, 2nd ed.; Wiley: New York, 1994.
(25) Nuzzo, R. G.; Fusco, F. A.; Allara, D. L. *J. Am. Chem. Soc.* **1987**, *109*, 2358.
(26) Porter, M. D.; Bright, T. B.; Allara, D. L.; Chidsey, C. E. D. *J. Am. Chem. Soc.* **1987**, *109*, 3559.

**Table 1.** Infrared Spectral Assignments for **1**

| frequency ($cm^{-1}$) | | |
|---|---|---|
| bulk **1** in KBr | SAM of **1** on Au | assignments[a] |
| 2917 | 2917 | $CH_2$, asym str |
| 2853 | 2849 | $CH_2$, sym str |
| 1722 | 1745 | C═O str |
| 1707[b] | | |
| 1622 | 1626 | ring C═C str |
| 1558 | 1559 | |
| 1511 | 1509 | |
| 1471 | 1477 | $CH_2$ scissor |
| 1396 | 1394 | α-$CH_2$ def and other modes? |
| 1291 | 1284 | C(C═O)−O asym str |
| 1238 | 1236 | ═C−O−C asym str |
| 1190 | 1200 | $CH_2$ wag and twist |
| 1143 | 1161 | C(C═O)−O sym str |
| 1133 | 1129 | $CH_2$ wag and twist |
| 1102 | 1099 | ═C−O−C sym str |
| 842 | 846 | ═C−H out-of-plane def |
| 824 | 835 | |

[a] The following symbols are used: str for stretching, sym for symmetric, asym for asymmetric, def for deformation. [b] Fermi resonance.

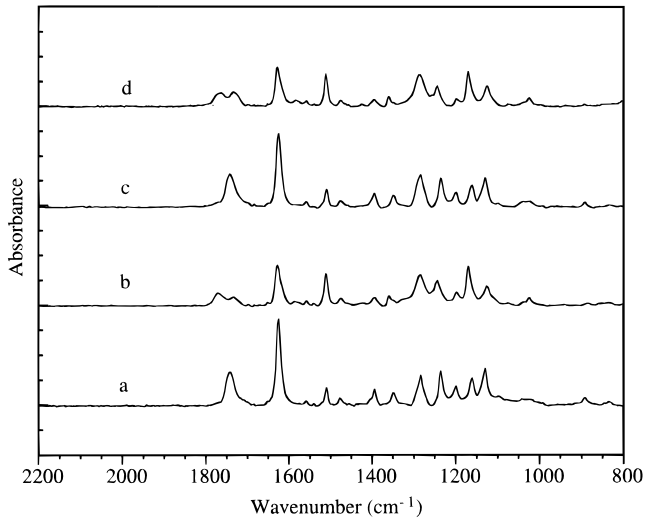


**Figure 4.** Continuous monitoring of the grazing angle surface FTIR spectra of Au-**1**: (a) before photodimerization; (b) after photodimerization; (c) after photocleavage; (d) again after a second photodimerization.

spectrum of **1** in KBr and the grazing angle surface IR spectrum of Au-**1**. The differences in line shapes and peak frequencies arise from the differences in orientational ordering and intermolecular interactions in the self-assembled monolayer and the bulk crystalline phase. The differences in relative intensity are due to differences in transition dipole moments between the monolayer and bulk solid phase.[25] The bands at 2918 and 2848 $cm^{-1}$ in the surface FTIR spectrum are assigned to the $\nu_a$ and $\nu_s$ $CH_2$ modes, respectively. The peak frequency of the $\nu_a(CH_2)$ mode provides information about packing of the long alkyl chains. The peak at 2918 $cm^{-1}$ indicates that Au-**1** adopts an arrangement with the long alkyl chains largely fully extended in an *all-trans* conformation.[26]

An Au-**1** sample was continuously monitored by grazing angle surface FTIR to investigate the changes induced by photodimerization and photocleavage. Figure 4 shows a grazing angle surface FTIR spectrum of Au-**1** before photodimerization, after photodimerization induced by irradiation at 350 nm, after photocleavage induced by the irradiation at 300 nm, and after a second photodimerization. Three changes induced by photodimerization are evident. First, the sharp C═O stretching vibration at 1745 $cm^{-1}$ is split into two peaks at 1771 and 1733 $cm^{-1}$; second, the intensity of the 1509 $cm^{-1}$ ring C═C stretching vibration more than doubled; third, three bands at 1200, 1161, and 1129 $cm^{-1}$ are shifted to 1197, 1170, and 1126 $cm^{-1}$. Upon photocleavage, the spectrum reverts completely to that of Au-**1** in band shape, peak frequency, and relative intensity. For example, the relative intensities of the bands at 1200, 1161, and 1129 $cm^{-1}$ are 1.0:1.5:2.1 in Figure 4c and 1.0:1.4:2.0 in Figure 4a.

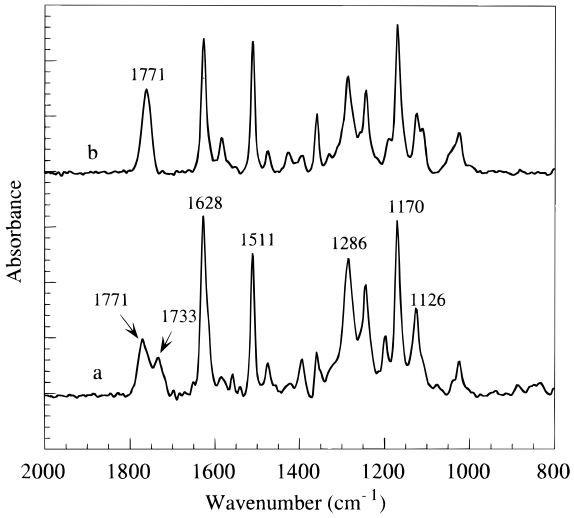


**Figure 5.** Grazing angle surface FTIR spectra of monolayer: (a) $(Au\text{-}\mathbf{1})_{dimer}$ after photodimerization and (b) Au-**2**

It is surprising to find nearly complete recovery of the monomer (Figure 4c) upon photocleavage of the photodimerized SAM induced by 300 nm light irradiation. In analogous coumarin derivatives and in the parent coumarin, photodimerization and photocleavage proceeded simultaneously in dispersed polymers[12] upon irradiation at 254 nm, ultimately approaching a photostationary state. In the absence of air, the Au−S−R linkage is quite stable toward our experimental conditions. After four photodimerization and photocleavage cycles, no photodegradation of the SAM was evident from FTIR measurements or from the electrochemical blocking effect of $Fe(CN)_6^{3-}$. However, when the photocleavage was done without the protection of an inert atmosphere or when the modified gold plate is in contact with a solvent, irradiation at 300 nm did eventually degrade the SAM.

In our studies the frequency for the $\nu_a(CH_2)$ mode remains constant at 2918 $cm^{-1}$ within experimental error (±1 $cm^{-1}$), showing that irradiation at neither 350 nm nor at 300 nm can induce disorder in the packing of the long alkyl chains. Although only two cycles are shown in Figure 4, four photocycles caused no detectable decomposition of Au-**1**, as judged by grazing angle surface FTIR spectroscopy.

The grazing angle surface FTIR spectrum of the monolayer prepared by irradiation of Au-**1**, i.e., $(Au\text{-}\mathbf{1})_{dimer}$, was compared with that observed by forming a monolayer from the *syn* H-H photodimer (**2**), i.e., Au-**2** in Figure 5. Except for the difference in carbonyl absorptions, the two spectra are nearly identical in band shape, peak frequency, and relative intensity. The carbonyl stretch in the *syn* H-H dimer (**2**) is a singlet at 1771 $cm^{-1}$, shifted to higher frequency from the monomer (1745 $cm^{-1}$), as expected from the loss of conjugation upon photodimerization.[27] The higher frequency band (1771 $cm^{-1}$) in the C═O absorption doublet from $(Au\text{-}\mathbf{1})_{dimer}$ is thus due at least partially to the C═O stretch from a *syn* H-H dimer, but another regioisomer must also be present. In principle, photodimerization of Au-**1** can produce only two (*syn* H-H and *syn* H-T, Scheme 3) of the four

(27) Silverstein, R. M.; Bassler, G. C.; Morrill, T. C. *Spectrometric Identification of Organic Compounds*; Wiley: New York, 1981.

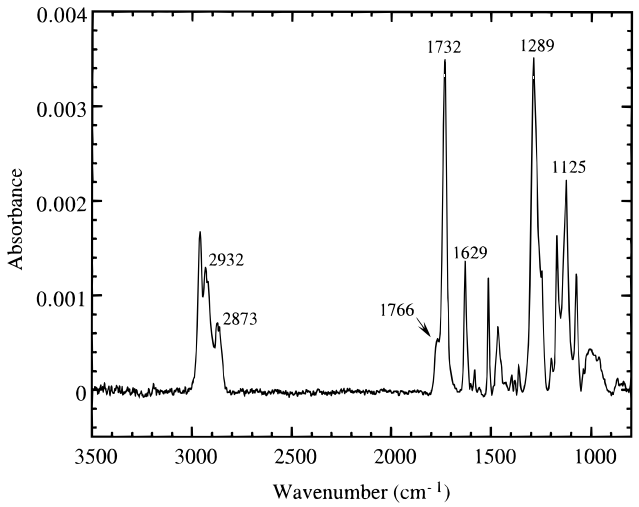


**Figure 6.** Grazing angle surface FTIR spectrum of monolayer (Au-**1**)$_{dimer}$ after photodimerization in contact with benzene, bubbling with $N_2$.

**Scheme 3**

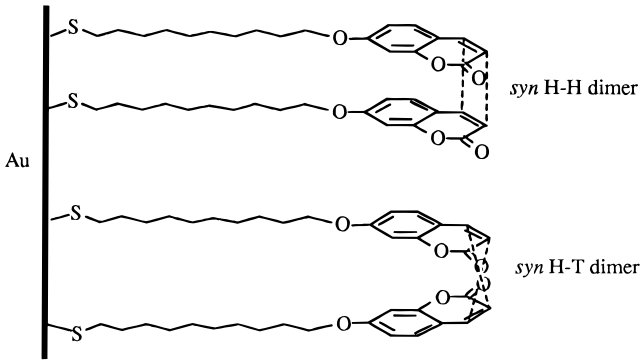


possible regioisomeric dimers because the *anti* dimers are likely inaccessible because of the conformational anchoring of the alkyl chain ends to the gold surface. Since the photodimerization might not proceed to 100% completion, some fraction of the unreacted monomer (1745 cm$^{-1}$) may be left in the largely photodimerized SAM. Therefore, either an *syn* H-T dimer or an unreacted monomer must be responsible for the lower frequency carbonyl absorption at 1733 cm$^{-1}$ in (Au-**1**)$_{dimer}$ (Figure 5a).

When Au-**1** was irradiated at 350 nm while in contact with $N_2$-saturated benzene, a dramatically different grazing angle surface FTIR spectrum was recorded (Figure 6) compared to that obtained when Au-**1** was not in contact with a liquid. The carbonyl stretch is nearly a singlet at 1732 cm$^{-1}$ (a very small peak at 1766 cm$^{-1}$ is due to carbonyl stretching of *syn* H-H dimer of Au-**1**). This value is identical to the lower frequency carbonyl absorption band in Figure 5a, within experimental error ($\pm$1 cm$^{-1}$). It is therefore tempting to assign the lower frequency carbonyl absorption at 1733 cm$^{-1}$ (Figure 5a) to the C═O stretch of an *syn* H-T dimer. The relative intensities of the peaks in the spectrum for the *syn* H-T dimer are also significantly different from those of the *syn* H-H dimer, particularly at 1732, 1629, and 1289 cm$^{-1}$. Unfortunately, attempts to synthesize independently the *syn* H-T dimer of **1** in $CH_2Cl_2$ were unsuccessful, possibly because of the interference by thiol photochemistry.[28]

In SAMs, if the methylene groups are in an extended *all-trans* alkyl chains, they will not be addressed by p-polarized light and thus will not appear in the IR spectrum. Only those in the alkyl chains tilted from the normal to the plane, the symmetric and asymmetric vibrations of the methylene groups, will appear in grazing angle spectra.[29] In contrast to the photodimerization of dry Au-**1** (without a contacting solvent), the peak intensities of the symmetric and asymmetric stretching of $CH_2$ increased significantly (over 12 cm$^{-1}$).[26] This suggests that the photodimerization of Au-**1**, when conducted in contact with benzene, induced disordering of the long alkyl chains, resulting in tilting from the normal to the gold surface. Photocleavage induced by irradiation of (Au-**1**)$_{dimer}$ at 300 nm while in contact with $N_2$-saturated benzene showed poor recovery of the monomer Au-**1** and photodecomposition was observed in the grazing angle surface FTIR spectrum. In contrast, good recovery of monomer is obtained for the same (Au-**1**)$_{dimer}$ by photocleavage under $N_2$.

**Table 2.** Advancing Contact Angles $\theta_a(H_2O)$ of water on SAMs of Au-**1**, (Au-**1**)$_{dimer}$, and Au-**2**

| surface | $\theta_a$ ($H_2O$) (deg, $\pm$1°) |
|---|---|
| Au-**1** | 58 |
| (Au-**1**)$_{dimer}$[a] | 63 |
| Au- **2** | 62 |

[a] Generated by direct irradiation of Au-**1** at 350 nm for 10 h under ambient conditions under $N_2$ without contact with benzene.

In summary, photodimerization of Au-**1** as a solid monolayer under $N_2$ results in both *syn* H-H (major) and *syn* H-T dimers, as shown by two C═O stretching absorption bands produced by the photodimerization (Figure 5) in which the higher frequency band (at 1771 cm$^{-1}$) is assigned to *syn* H-H dimer and the lower frequency absorption (at 1733 cm$^{-1}$) is assigned to *syn* H-T dimer. Most intervening alkyl chains are perpendicular to the surface. However, photodimerization of Au-**1** while in contact with benzene results in predominant *syn* H-T dimer formation, with the alkyl tails remaining more disordered and tilted significantly from the normal of the surface, probably because the benzene solvates the coumarin rings exposed at the outside surface and permits easier conformational flexing. The disordering of the alkyl tails in the *syn* H-T dimer, but not in the *syn* H-H dimer, can be best rationalized by molecular modeling. In the energy-minimized structure of *syn* H-H dimer, minimal conformation changes in alkyl tails are required, since the two alkyl tails in the *syn* H-H dimer can still adopt a close-packed, *all-trans* conformation. Formation of the energy-minimized structure of the *syn* H-T dimer, on the other hand, requires significant reorganization of the two alkyl tails, which cannot both adopt a close-packed, *all-trans* conformation, resulting in disordering and tilting of the alkyl methylene groups.

**Contact Angle Measurements.** Sessile drop contact angle measurements are known to be extremely sensitive to surface composition.[30] Theoretically, all metal surfaces are hydrophilic, which should result a very small contact angle $\theta_a$ with $H_2O$. However, under ambient lab conditions, a sessile contact angle $\theta_a(H_2O)$ for a clean gold surface has been reported to range from 30 to 70°,[18] probably because freshly prepared gold surfaces are easily contaminated by hydrophobic species physisorbed from laboratory air.[30]

Table 2 summarizes the contact angles of water on Au-**1**, (Au-**1**)$_{dimer}$, and Au-**2** monolayers. The contact angle $\theta_a(H_2O)$ for a hydrophilic SAM of $HS(CH_2)_{11}OH$ on Au is <10°, whereas that of a hydrophobic SAM of $HS(CH_2)_nCH_3$ ($n > 5$) on Au is 110−114°.[18] A contact angle $\theta_a(H_2O)$ of Au-**1** of 58° is consistent with the exposure of a polar ester group from the coumarin rings at the surface.

(28) Whitham, G. H. *Organosulfur Chemistry*; Oxford University Press, Inc.: New York, 1995.

(29) Ulman, A. *An Introduction to Ultrathin Organic Films: From Langmuir−Blodgett to Self-assembly*; Academic Press: Boston, MA, 1991.

(30) Schrader, M. E.; Loeb, G. I. *Modern Approaches to Wettability: Theory and Applications*; Plenum Press: New York, 1992.

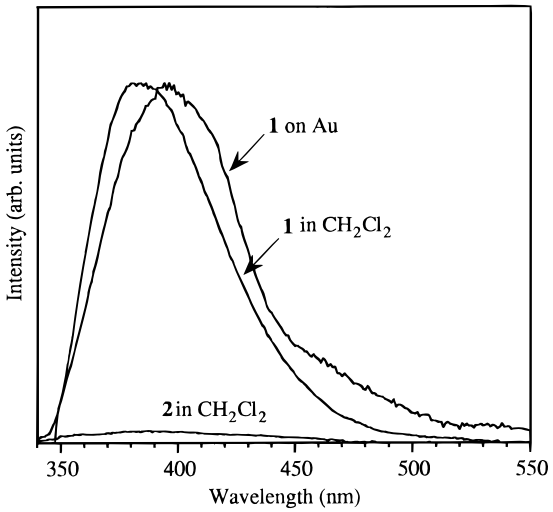


**Figure 7.** Emission spectra of degassed solutions of **1** and **2** in $CH_2Cl_2$ ($10^{-5}$ M) and of Au-**1** (normalized to 396 nm), excitation at 320 nm.

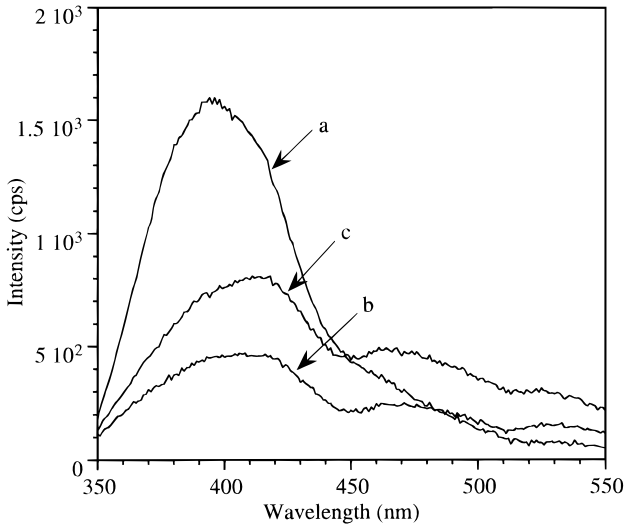


**Figure 8.** Fluorescence spectra for Au-**1**: (a) before photodimerization; (b) after photodimerization; (c) after photocleavage.

Changes in contact angle induced by photodimerization and photocleavage were also investigated. After 1 h of irradiation at 350 nm under $N_2$, the contact angle of Au-**1** increases to 63°, indicating a slightly more hydrophobic surface after photodimerization than before. This value is virtually identical with the contact angle $\theta_a(H_2O)$ of 62° for the *syn* H-H dimer on gold (Au-**2**), within experimental error (±1°). This is consistent with a pair of conjugated esters being replaced by a less polarizable, more hydrophobic simple ester bound to a cyclobutane ring in the photodimer. For example, the contact angle $\theta_a(H_2O)$ of the SAM of $HS(CH_2)_{17}CH{=}CH_2$ on Au is 107°, and that of $HS(CH_2)_{21}CH_3$ is 112°.[18] The contact angle for $(Au\text{-}\mathbf{1})_{dimer}$ remains unchanged within experimental error (±1°) upon further irradiation at 350 nm, indicating that no further photodecomposition takes place under these experimental conditions. After the photodimers were photocleavaged at 300 nm, the observed contact angle returned to the original value (58°), indicating good reversibility of the photodimerization by photocleavage, as was indicated by IR spectra (see above).

**Fluorescence Studies.** Upon excitation at 320 nm, monomer **1** shows strong fluorescence emission (Figure 7) at 384 nm. In contrast, at this same wavelength *syn* H-H dimer (**2**) absorbs only weakly and consequently displays only very weak fluorescence (less than 3% of the intensity of **1** in solution) and that is likely due to residual contamination from **1** (<1%). Au-**1** presents a similar fluorescence emission profile to that of **1** in solution, except for a red-shift of about 10 nm. Such red-shifts are more common for fluorescence spectra in solution than in the solid state.[31] The fluorescence excitation spectrum of Au-**1** and the solution phase absorption spectrum of **1** in $CH_2Cl_2$ are nearly identical, with maxima at 323 nm. On the other hand, nearly no fluorescence could be observed either from Au-**2** or from the *syn* H-H dimer **2** upon excitation in this wavelength region.

Fluorescence emission and excitation spectra thus directly point to the presence of coumarin chromophores in an environment where it is not quenched by electronic interaction with the gold surface. Both the emission and excitation spectra of Au-**1** are reasonably intense (>1500 cps), despite the known efficiency of nonradiative energy transfer from excited molecules to a metal surface across 10 nm thick Langmuir−Blodgett films.[16,32]

Surface fluorescence was employed to study the emission of Au-**1**, $(Au\text{-}\mathbf{1})_{dimer}$, and its photoreversion product during different stages of the photodimerization and photocleavage cycle. Figure 8 shows the fluorescence spectra observed during one photodimerization−reversion cycle for Au-**1**. The emission intensity of Au-**1** at 394 nm dropped more than 60% upon photodimerization. However, upon photocleavage, only about 60% of the original monomer emission recovered. Since the grazing angle surface FTIR studies demonstrated a full recovery of monomer upon photocleavage in four cycles, this observation suggest that the coumarin monomers obtained from photodimers are found in an environment somewhat different from the coumarin monomers present in the original Au-**1** SAM. Perhaps the coumarin monomers generated from the cleavage of the photodimers may remain in a face-to-face conformation, which might facilitate self-quenching or stronger electronic coupling to the gold surface. In any case, the new band at 470 nm produced upon irradiation is not easily depleted by shorter wavelength irradiation. Despite the good reversibility of the photodimerization, practical attempts to record photopatterning of the Au-**1** surface by fluorescence microscopy based on irradiated and nonirradiated area (Olympus iX-70 fluorescence microscope) have not yet been successful, because of the low contrast of the pattern (nonirradiated area) with respect to the background (irradiated area).

## Conclusions

Self-assembled monolayers of 7-(10-thiodecoxy)coumarin (**1**) and its *syn* head-to-head dimer (**2**) on a polycrystalline gold have been prepared and characterized. Through FTIR spectra, sessile drop contact angle measurements, and surface fluorescence studies, we have demonstrated that reversible photodimerization of **1** occurs in the monolayer.

**Acknowledgment.** This research has been supported by the U.S. Department of Energy, Office of Basic Energy Science, and the Robert A. Welch Foundation. We are grateful to Professor Stephen Webber for use of his fluorometer.

JA970633M

(31) Rabek, J. F. *Mechanisms of Photophysical Processes and Photochemical Reactions in Polymers: Theory and Applications*; Wiley: New York, 1987.

(32) Pockrand, I.; Brillante, A.; Möbius, D. *Chem. Phys. Lett.* **1980**, *69*, 499.